MEAN FLOW PROPERTIES IN THE DEVELOPING REGION OF A CIRCULAR PIPE FOR TURBULENT FLOW AT MAXIMUM DRAG REDUCTION

By

M. H. EMBABY and A. VERBA

Department of Mechanical Engineering for the Chemical Industry,
Technical University, Budapest

Received October 1, 1979

Introduction

Prediction of Newtonian turbulent flow properties in the developing region of a pipe has been dealt with by many authors [1], [6]. While such predictions for conditions of drag reduction seem not to be available, extensive studies have been published on the fully developed flow properties [2], [4]. In a trial to predict the effect of drag reduction conditions on the developing flow properties, a model for maximum drag reduction is adopted in the following analysis. The mathematical treatment followed in [1] is also adopted with the previous model of maximum drag reduction [2].

Analysis

The momentum integral method for predicting the developing region of a circular pipe is the following:

Consider the model of boundary layer development shown in Fig. 1. Take a force balance in the longitudinal direction across an element of length dx of the boundary layer of thickness δ.

Thus:

$$-\tau_w \cdot D \cdot dx - dP \cdot \delta \cdot (D - \delta) = 2d\left[\int_{R-\delta}^{R} \varrho u^2 \cdot r \cdot dr\right] - 2 \cdot U_G d\left[\int_{R-\delta}^{R} \varrho u r dr\right] \quad (1)$$

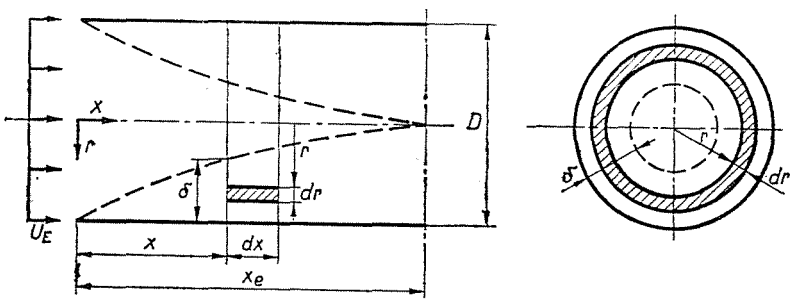

Fig. 1. Descriptive sketch of analysis symbols

with $dP = -\varrho U_G dU_G$ in the core, substituting and rearranging gives:

$$\frac{dx}{D} = \frac{2}{\tau_w D^2} \cdot \frac{\varrho U_G}{2} \cdot \delta \cdot (D - \delta)\, dU_G + U_G \frac{2\varrho}{\tau_w D^2} \cdot d\left[\int_{R-\delta}^{R} urdr\right] - \frac{2\varrho}{\tau_w D^2} d\left[\int_{R-\delta}^{R} u^2 r dr\right].$$

In dimensionless form, using the notations p. 91, integrating from 0 to x:

$$\frac{X}{D} \int_{U_E^+ D_{E^+}}^{U_G^+ D^+} \left[\frac{U_G^+}{D^{+3}}(D^+ - \delta^+)\,\delta^+ - \frac{2}{D^{+3}} \int_{R^+-\delta^+}^{R^+} u^+ r^+ dr^+\right] d(U_G^+ D^+ +)$$
$$+ \int_a^b \frac{2}{D^{+2}} d\left[\int_{R^+-\delta^+}^{R^+} (U_G^+ - u^+]\, u^+ r^+ dr^+\right]. \qquad (3)$$

Where the limits "a" and "b" represent the variables of the second integral at both the entrance and X.

To evaluate the integrals in Eq. (3); D^+ is required to be known in terms of δ^+ and u^+ in terms of r^+.

$D^+ - \delta^+$ relation:

Continuity requires the average velocity U_M to remain the same along the pipe; thus:

$$\pi \cdot \varrho \cdot U_M \cdot \frac{D^2}{4} = 2\pi \int_{R-\delta}^{R} \varrho \cdot u \cdot r \cdot dr + \varrho \cdot U_G \cdot \frac{\pi}{4}(D - 2\delta)^2$$

or, in dimensionless form:

$$U_M^+ D^+ = \frac{8}{D^+} \int_{R^+-\delta^+}^{R^+} u^+ r^+ dr^+ + \frac{U_G^+}{D^+}(D^+ - 2\delta^+)^2 . \qquad (4)$$

Velocity profile model (Fig. 2).

The model of dimensionless velocity profile suggested by Virk [2] for fully developed turbulent flow at maximum drag reduction is adopted here. This model assumes a viscous sublayer and an elastic layer completely filling the pipe. Thus this model is represented by the line OA3 in Fig. 2b. However, concerning the velocity profiles in the developing zone, the following asumptions are stated:

I At the entrance the velocity distribution is uniform.

II The contributions by the viscous sublayer to the integrals in Eqs (3) and (4) are negligible compared to those by the elastic layer.

III The turbulent elastic layer begins to develop at the entrance with zero thickness until full development with thickness of half the pipe diameter. Thus, at any section there is an elastic layer of thickness δ and a core of uniform velocity U_G (section 2 in Fig 2a and line OA2 in Fig 2b).

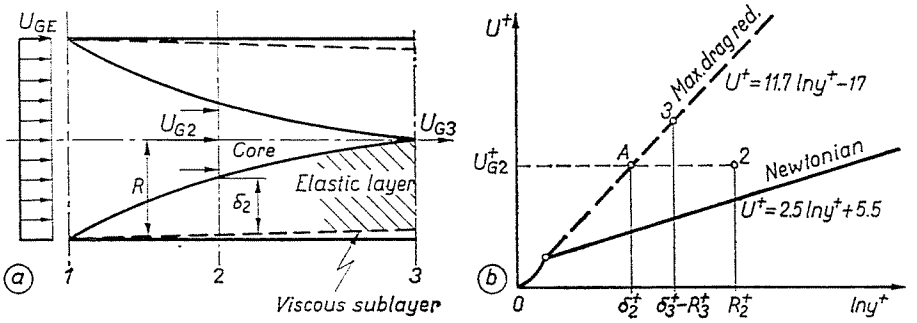

Fig. 2. Suggested velocity profiles

IV The dimensionless velocity profile in the developing layer δ, normalized by its local shear velocity, is similar to that prevailing in the fully developed flow (line OA in Fig. 2b).

Accordingly, the velocity profile at any section will be:

For maximum drag reduction:

$$\left.\begin{aligned} u^+ &= 11.7\ln y^+ - 17 && 0\leq y^+\leq\delta^+ \\ u^+ &= U_G^+ = 11.7\ln\delta^+ - 17 && \delta\leq y^+\leq R^+ \end{aligned}\right\}. \tag{5.a}$$

For Newtonian fluids, the well-known logarithmic velocity profile:

$$\left.\begin{aligned} u^+ &= 2.5\ln y^+ + 5.5 && 0\leq y^+\leq\delta^+ \\ u^+ &= 2.5\ln\delta^+ + 5.5 && \delta^+\leq y^+\leq R^+ \end{aligned}\right\}. \tag{5. b}$$

Friction factor correlation:

Since the Reynolds number is:

$$R_e = \frac{U_M D}{\nu} = U_M^+ D^+. \tag{6}$$

Defining the local friction factor C_f as:

$$C_f = \tau_w/0{,}5\ \varrho U_M^2.$$

Using Eq. (6) yields:

$$C_f/2 = D^{+2}/R_e^2. \tag{7}$$

Procedure of calculation:

Substituting Eq. (6) on the L. H. S. of Eq. (4) yields:

$$R_e = \frac{8}{D^+}\int_{R^+-\delta^+}^{R^+} u^+ r^+ dr^+ + \frac{U_G^+}{D^+}(D^+ - 2\delta^+)^2. \tag{8}$$

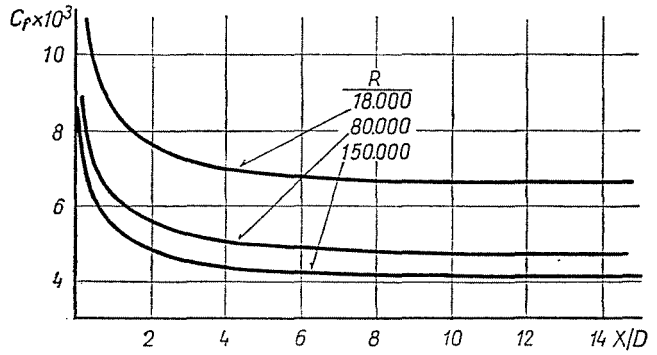

Fig. 3. Local coefficient of friction distribution (newtonian fluids)

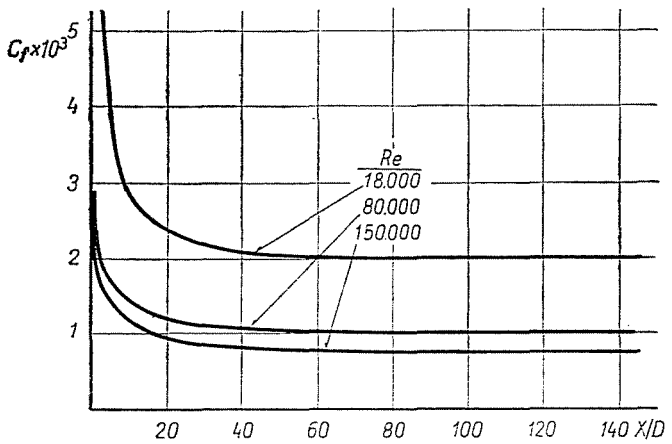

Fig. 4. Contd. (maximum drag reduction)

Thus the friction factor C_f can be evaluated as a function of the distance from entrance X/D. At a certain Reynolds number Re for a certain value of δ^+, Eq. (8) gives the corresponding D^+ value.
These values are used to evaluate the local friction factor C_f, Eq (7), and the elements of the integrals in Eq. (3). Integrations were carried out numerically and the results are shown in Fig. 3 for Newtonian flow and in Fig. 4 for maximum drag reduction.

Prediction of the dimensionless static pressure distribution in the entrance region:

In the core, the momentum balance gives:

$$dP = -\varrho U_G dU_G$$

which upon integration, in dimensionless form gives:

$$\Delta\overline{P}\Big|_{X/D} = \frac{P_E - P}{0{,}5\,\varrho U_M^2} = \left(\frac{U_G^+ D^+}{R_e}\right)^2\Bigg|_{X/D} - 1\,. \tag{9}$$

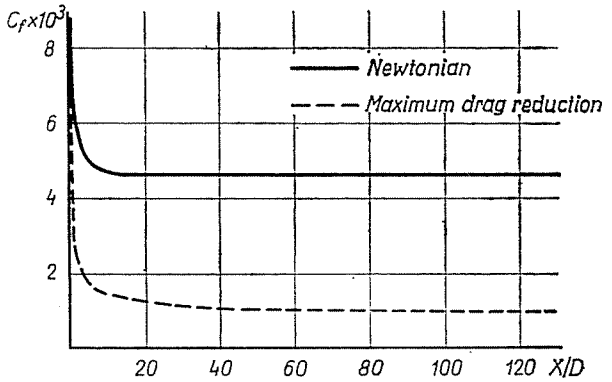

Fig. 5. Local coefficient of friction distribution, Re = 80.000

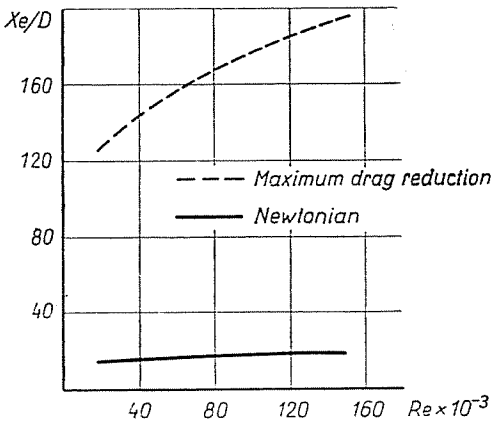

Fig. 6. Dimensionless entrance length (Xe/D) vs. Re

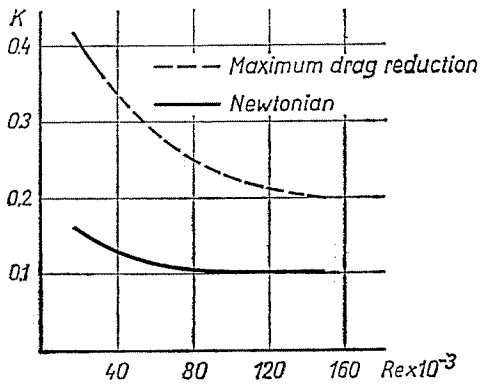

Fig. 7. Incremental pressure drop factor K vs. Reynolds number "Re"

The calculation results are shown in Figs 8, 9 and 10.

Prediction of the entrance length Xe/D:

Assuming fully developed velocity profile, where D^+ is twice δ^+, Eq. (8) is used to determine this value of δ^+. Then, the corresponding Xe/D is obtained. The results are shown in Fig. 6.

Prediction of the incremental entrance pressure drop factor K:

Using the definition, in [3],

$$K = \Delta P_e / 0{,}5 \varrho U_M^2.$$

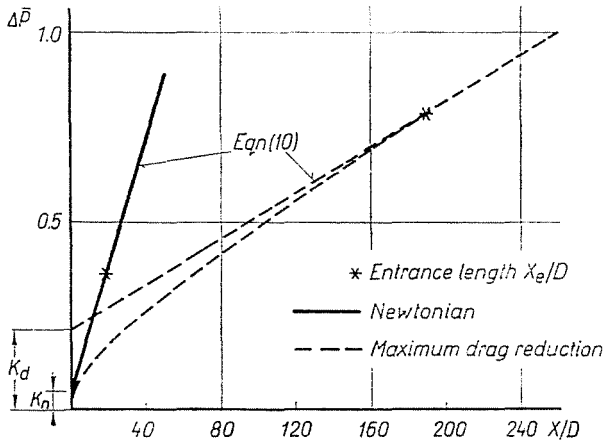

Fig. 8. Dimensionless static pressure drop distribution Re = 18000

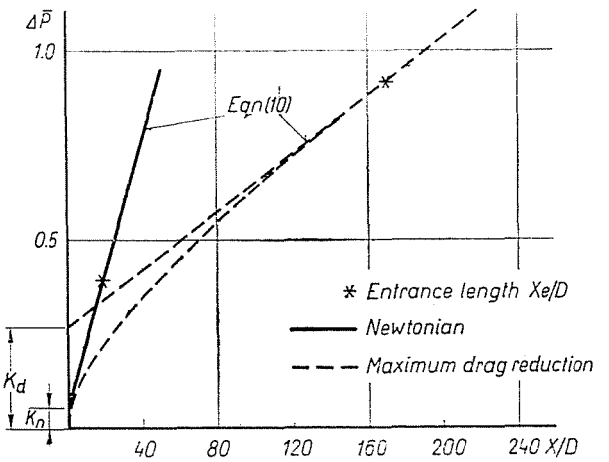

Fig. 9. Contd., Re = 80.000

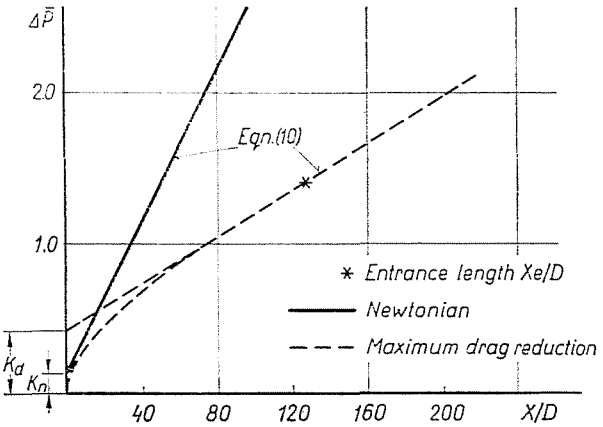

Fig. 10. Contd., Re = 150.000

Thus, at any point in the fully developed flow region, $X/D \geq Xe/D$ the relationship

$$\Delta\bar{P}\Big|_{X/D} = 4C_{f,fd}\, X/D + K, \quad X/D \geq X_e/D \tag{10}$$

holds.

At $X/D = Xe/D$, both Eqs (9) and (10) hold, and then K is calculated from:

$$K = \left(\frac{U_G^{+}\, D^{+}}{R_e}\right)^2\Bigg|_{X_e/D} - 4C_{f,fd}\,\frac{X_e}{D} - 1. \tag{11}$$

The calculation results are shown in Fig. 7.

Approximate representation of the static pressure distribution along the pipe:

Using the previous predictions of both K and Xe/D with the fully developed coefficient of friction $C_{f,fd}$, the dimensionless static pressure distribution along the pipe can be determined. Thus, the straight line represented by Eq. (10) determines the pressure distribution in the fully developed region $X/D \geq Xe/D$. The pressure distribution in the entrance zone is then the curve passing through the origin and having the previous straight line as a tangent at $X/D = Xe/D$ (Figs 8, 9 and 10).

Discussion

Predictions of the local coefficient of friction and static pressure distributions along the pipe, the entrance length and the incremental entrance pressure drop for turbulent flow with maximum drag reduction are presented. Similar

predictions for the Newtonian case are presented and comparison is made. The calculation results for different Reynolds numbers are shown in Figs 3 to 10. The figures show that:

I: Local coefficient of friction C_f
For both Newtonian and maximum drag reduction flow conditions, the local coefficient of friction distribution along the pipe has the same trend (Figs 3 and 4).
As the Reynolds number increases, the local coefficient of friction decreases (Figs 3 and 4).
For the same Reynolds number, at any section X/D, the local coefficient of friction is less in case of maximum drag reduction than of Newtonian flow (Fig. 5.).

II: The dimensionless static pressure distribution $\Delta\bar{P}$: For both Newtonian and maximum drag reduction conditions, $\Delta\bar{P}$ decreases with the increase of the Reynolds number (Figs. 8, 9 and 10).
In case of drag reduction for the same Re, at any section X/D, $\Delta\bar{P}$ is less than that for Newtonian flow. (Figs. 8, 9 and 10).

III: The entrance length Xe/D (Fig 6).
For the same Reynolds number, Xe/D is higher under conditions of maximum drag reduction than of Newtonian flow.
The figure also shows that as the Reynolds number increases Xe/D has a steeper ascent in the case of max. drag reduction.

IV: The incremental entrance pressure drop factor K (Fig. 7).
For the same Reynolds number K appears from the figure to be higher under conditions of maximum drag reduction.
The figure also shows that as Reynolds number increases K decreases with a steeper slope in case of max. drag reduction.

Physical interpretation

Since under the conditions of drag reduction U_G/U_M is higher than that in the Newtonian case, this qualitatively requires a longer length X_e to fully develop. Also the incremental entrance pressure drop due to integrated excess local shear stresses and flow acceleration in the entrance zone is qualitatively higher in the case of drag reduction. This is because — although the excess local shear stresses are less than Newtonian, — the limit of integration X_e is higher. Besides the flow acceleration is higher than Newtonian. Thus the quantitative predictions presented here have been physically supported.

Conclusions

I. At a certain Reynolds number, the local coefficient of friction, and the static pressure distribution along the pipe have the same trend for both Newtonian and maximum drag reduction flows.

II. At a certain Reynolds number, at any section along the pipe, both the local coefficient of friction and the pressure drop are less under conditions of maximum drag reduction than those under Newtonian flow conditions. Thus the drag reduction exists both at the entrance and the fully developed flow regions.

III. In case of flow with maximum drag reduction for a certain Reynolds number both the entrance length and the incremental entrance pressure drop are higher than those for Newtonian flow.

Notations

C_f:	friction factor defined in Eq. (7);
D:	pipe diameter;
K:	incremental entrance pressure drop factor defined in Eq. (10);
P, ΔP_e, $\overline{\Delta P}$:	pressure, incremental pressure drop due to entrance effects, nondimensional pressure drop, respectively;
r, R:	radial distance, pipe radius;
R_e:	Reynolds number defined in Eq. (6);
u, $u^* = \sqrt{\tau/\varrho}$	axial velocity, local shear velocity;
U_E, U_G, U_M:	velocities at the entrance; outside the boundary layer, mean, resp.;
X, X_e:	axial coordinate, entrance length;
$y = R - r$	distance from the pipe wall;
δ:	boundary layer thickness;
ν:	kinematic viscosity of Newtonian fluid or of solvent in case of drag reduction;
ϱ:	mass density;
τ:	shear stress;
	Velocity superscript $+$ implies: velocity/u^*.
	Length superscript $+$ implies: length $\cdot\, u^*/\nu$
	Subscripts:
d:	evaluated at conditions of maximum drag reduction;
fd:	evaluated in the fully developed flow;
n:	evaluated for Newtonian flow;
w:	evaluated at pipe wall;
E:	evaluated at entrance.

Summary

A theoretical analysis is given for the prediction of the mean flow properties in the developing region of a circular pipe for turbulent flow at maximum drag reduction. By comparison with the Newtonian flow, the analysis points to a drag reduction in both the entrance and the fully developed flow regions. On the other hand, the effect of drag reduction conditions is to increase the entrance length and the incremental entrance pressure drop.

References

1. AHMED, S. and BRUNDRETT: Int. J. Heat and Mass Transfer, vol. 14, pp. 365—375, 1971.
2. VIRK, P. S.: AICHE J., vol. 21, No 4, pp. 625—656, 1975.
3. SALEM, E. and EMBABY M. H.: Applied Scientific Res. 33, 2, 119—139, 1977.
4. LUMLEY, T. L.: J. Poly. Sc. Macromolecular Reviews. 7, 263—290. 1973.
5. SEYER, T. A.: J. Fluid Mech. 40, 4, pp. 807—819, 1970.
6. KNUDSEN and KATZ: "Fluid Dynamics and Heat Transfer" McGraw Hill. 1958. p. 236.

Mohamed Hamed, EMBABY
Dr. Attila VERBA
} H-1521 Budapest